- Technical Paper -

SHEAR CRACKING BEHAVIOR OF ULTRA-HIGH-STRENGTH PRESTRESSED REINFORCED CONCRETE BEAMS

Sudhira DE SILVA[*1], Hiroshi MUTSUYOSHI[*2], Shingo ASAMOTO[*3], and Atsushi MAEKAWA[*4]

ABSTRACT

An experimental program was conducted to investigate the shear cracking behavior of both normal strength concrete and ultra-high-strength concrete I-shaped beams. All beams were tested by focusing on the influence of prestressing force and compressive strength of the concrete on the shear crack width. It was found that there is a linear relationship between shear crack width and stirrup strain in the both normal strength and ultra-high-strength concrete beams. Shear crack widths are smaller in ultra-high strength PRC beams.

Keywords: ultra-high-strength concrete, prestressing force, shear crack width, stirrup strain

1. INTRODUCTION

Cracking in concrete structures has received enormous research attention, as durability and serviceability of concrete structures are often dependent on crack formation. Excessive crack widths can impair corrosion resistance of structures exposed to the severe environment. Therefore, control of cracking is more important for serviceability.

Recently, the use of small and economic reinforced concrete sections has increased because of their simplicity [1]. Ultra high strength concrete (UHSC) is a new class of concrete that has recently been developed. Compared to normal strength concrete, UHSC tends to exhibit superior properties such as advanced strength, excellent durability, low permeability, low creep, and better workability encouraging design engineers to use UHSC [1, 2]. The high performance concrete is widely used today to emphasize that strength alone may not be the primary reason. Durability, particularly threatened by reinforcement corrosion, is the major issue world wide concern. Properly designed structures that used UHSC have the potential to delay deterioration processes and thereby prolong the service life of the structure.

In addition, UHSC has widely been used in construction filed because increased strength associated with UHSC provides a better solution to reduce size and weight of concrete in structural elements. Prestressed concrete beams incorporating with non-prestressed steel reinforcements are built today with an allowance of tension in concrete, which are well known as prestressed reinforced concrete (PRC) in Japan. Cracking behavior of reinforced concrete (RC) beams and PRC beams have been investigated over the last five decades by conducting comprehensive experiments [1-4]. The previous experimental studies conducted by the authors [3, 4] have investigated the effects of prestressing force, stirrup ratio, and side concrete cover on shear crack width of RC and PRC beams. More studies related to HSC are concerned on concrete strength range from 60 MPa to 80 MPa, but a few studies have been done with concrete strength of range between 100 to 160 MPa. It has been reported that the crack plane in UHSC is relatively smooth compared to that in normal strength concrete (NSC) as a crack passes through an aggregate in UHSC whereas a crack goes around an aggregate in NSC [2].

A characteristic of high strength concrete and ultra high strength concrete is a brittle failure mode. Moreover, due to the higher tensile strength of high strength concrete, a higher cracking shear is expected. Significant effects of concrete strength on shear capacity and properties of structural elements found in the previous studies [2-4] imply that concrete strength can have an influence on shear crack width, but there is no known study of the effect of concrete strength on shear crack width.

The recent study by the authors [4] has investigated the effect of high strength concrete with concrete compressive strength of 100 MPa on shear crack width of RC and PRC beams. Experimental results encouraged authors to further investigate the shear cracking behavior in ultra high strength concrete specimens. The objective of this study was to investigate the effect of ultra-high-strength concrete on shear cracking behavior of RC and PRC beams experimentally.

*1 PhD Student, Graduate School of Science and Engineering, Saitama University, JCI Member
*2 Professor, Graduate School of Science and Engineering, Saitama University, JCI Member
*3 Asst. Professor, Graduate School of Science and Engineering, Saitama University, JCI Member
*4 MEng Student, Graduate School of Science and Engineering, Saitama University, JCI Member

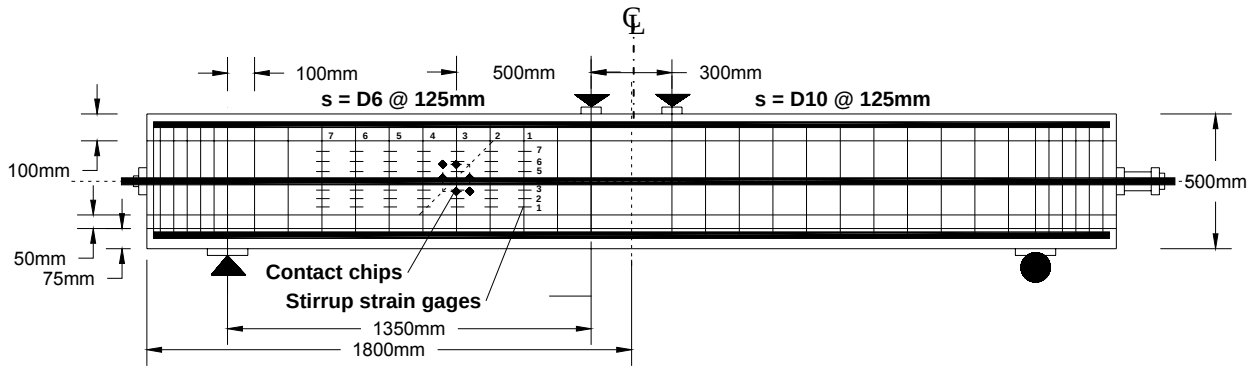

Fig. 1 Layout of the specimens

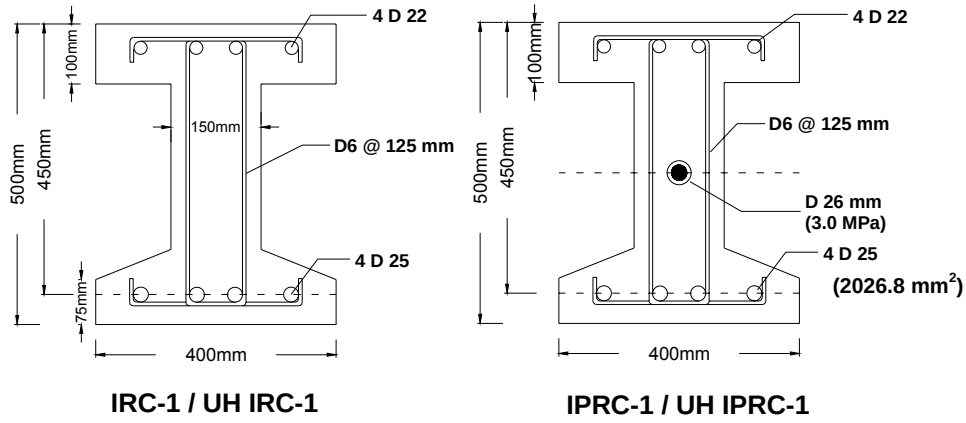

Fig. 2 Cross sectional details

Table 1 Experimental variables

Beam #	Non-prestressed reinforcement		Prestressing force (kN)	Type of concrete
	Top	Bottom		
IRC-1	4 D22 (ds'=40 mm)	4 D25 (ds=450 mm)	-	NSC
UH IRC-1				UHSC
IPRC-1			375.0 kN (3.0 MPa)	NSC
UH IPRC-1				UHSC

d_s' and d_s-distance to compression and tension r/f, respectively

Table 2 Mechanical properties of reinforcements

Type of bar	Φ (mm)	Type	*fy* (MPa)	Es x 10^3 (MPa)
Deformed bar	D6	SD 345	438	180
	D10		376	200
	D22		397	
	D25	USD 685	720	206
PC bar	26	SBPR 1080/1230	1205	200

2. EXPERIMENTAL PROGRAM

In order to investigate the influence of compressive strength of concrete including prestressing force on shear crack width in PRC beams, the following experimental program was carried out. The compressive strength of concrete was 40 MPa for normal strength concrete (NSC) specimens and that was 160 MPa for ultra-high strength concrete (UHSC) specimens at the age of 28 days under moist curing condition. Test specimens consisted of two RC and two PRC beams having I-shaped cross section. A total length of beam is 3600 mm. The typical layout and cross sectional details of the specimens are shown in Figs. 1 and 2, respectively. The experimental variables are summarized in Table 1. The mechanical properties of reinforcements used in the experiment are listed in Table 2. Table 3 shows concrete properties used. In all test specimens, stirrups were provided with two different sizes of stirrup bars; D6 bars were in the left span of the beams and D10 bars were in the right span of the beams. This arrangement of different sizes of bars was necessary so as to ensure that the main shear crack would occur in the left span of the beam. The four point symmetrical loading with a distance of 300 mm between the loading points (a/d of 3.0) was statistically applied to all specimens. Contact chips were pasted on the concrete surface at 500 mm from the left-loading point of the beam in the shear span region so as to measure the principal strains and their directions. A digital microscope, which has a precision of 0.001 mm, was used to capture digital photographs of the crack occurred in the left span of the beam (Fig. 3). The digital image captured at the crack location was used to measure the crack width. At three arbitrary extracted points, perpendicular to the crack surface at close to the location of necessity was measured. The average of measured three crack widths was used as the crack width at that location (Fig. 3b).

Table 3 Concrete properties

	NSC	UHSC
Average compressive strength of concrete (MPa)	41.7	173.1
Slump[a] / flowability[b] (mm)	174.0[a]	648.7[b]
Air content (%)	-	1.65
water / cement ratio	0.47	0.17
Tensile strength (MPa)	3.00	5.96
Young's modulus (GPa)	33.7	46.3

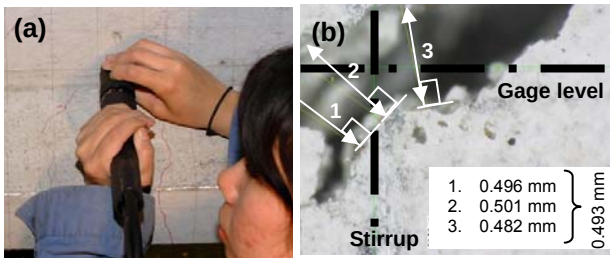

Fig. 3 (a) Measuring crack width by using digital microscope,
(b) Digital image of measured crack width

Table 4 Failure loads

Beam #	*f'c* (MPa)	Failure load (kN)	Failure mode
IRC-1	40.3	559.7	Shear failure without yielding tension reinforcements. All stirrups yield.
UH IRC-1	176.5	685.5	
IPRC-1	41.8	706.8	
UH IPRC-1	169.8	1052.3	

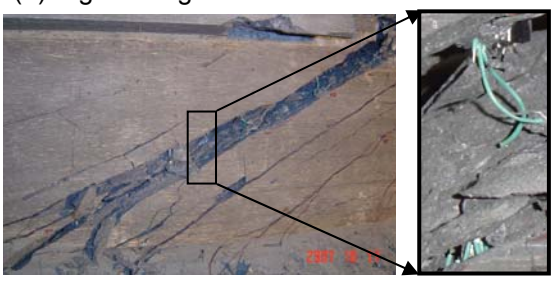

Fig. 4 Stirrup steel fracture through the failure shear crack

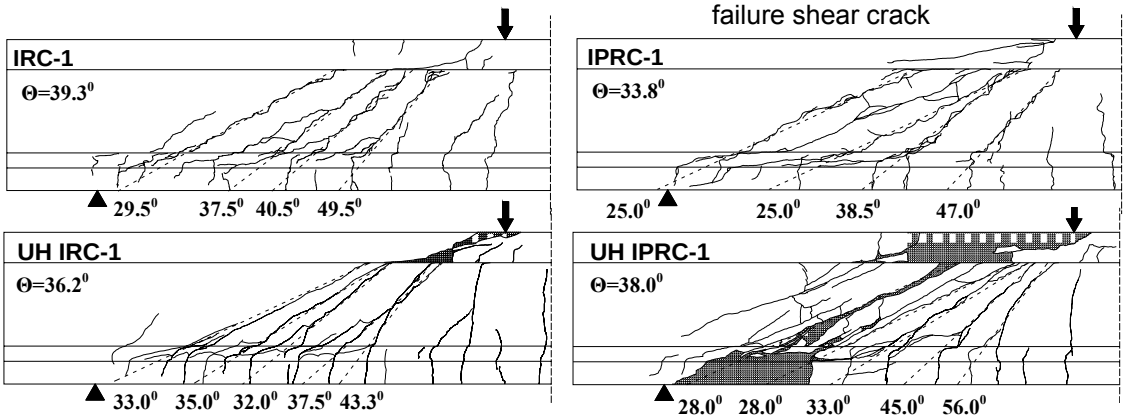

Fig. 5 Failure crack patterns and crack angles

3. TEST RESULTS AND DISCUSSION

3.1 Failure Mode and Crack Pattern

Crack patterns at failure for all specimens are shown in Fig. 5. All specimens failed in shear failure mode (Table 4) with wide shear cracks in the shear span region. The failure of ultra high strength concrete specimens show brittle behavior compared to normal strength specimens. The developments of initial flexural cracks are straight and crack height is more than half of the beam depth. Specimen UH IPRC-1 showed explosive failure mode with fractured stirrups along the main shear crack (see Fig. 4). It shows significant improve bond between the steel and the concrete in UHSC than NSC. The inclination of shear cracks was determined by averaging crack angle measured in the shear span region. It can be seen that in PRC beams the inclination of shear cracks slightly decrease due to prestressing force. The effect of strength of concrete on shear crack angle was insignificant. However, the number of shear cracks appeared in UHSC specimens was greater than that in NSC specimen. The spacing in between shear cracks was smaller in UHSC specimens. Specific discussion about shear crack spacing is given in section 3.4.

3.2 Effect of Compressive Strength of Concrete

In the case of high strength concrete and ultra-high-strength concrete it has been reported that large autogenous shrinkage can occur and shrinkage cracking can be appeared due to insufficient curing [2]. This study was carried out with proper moist curing. As a result, there were no shrinkage cracks appearing in UHSC specimens. Fig. 6 shows the relationship between shear force and maximum stirrup strain. It can be seen that a similar rate of increment in stirrup strain with increasing shear force in both NSC and UHSC specimens. Shear cracking load is higher in UHSC specimens compared to NSC specimen. After shear crack developed, specimen UH IPRC-1 shows larger stirrup strain. This is attributed to fact that, higher prestressing force and superior bond in UHSC with steel. Relation between shear force and maximum shear crack width is presented in Fig. 7. At a particular shear force, maximum shear crack width is almost similar in RC beams and PRC beams. Further, it was noticed that sudden growth in shear crack width in UHSC specimen. This is observed due to large entrap energy and brittle behavior of UHSC than NSC. Shear crack width and stirrup strain were measured at the same locations (see Fig. 1 for stirrup strain gage locations).

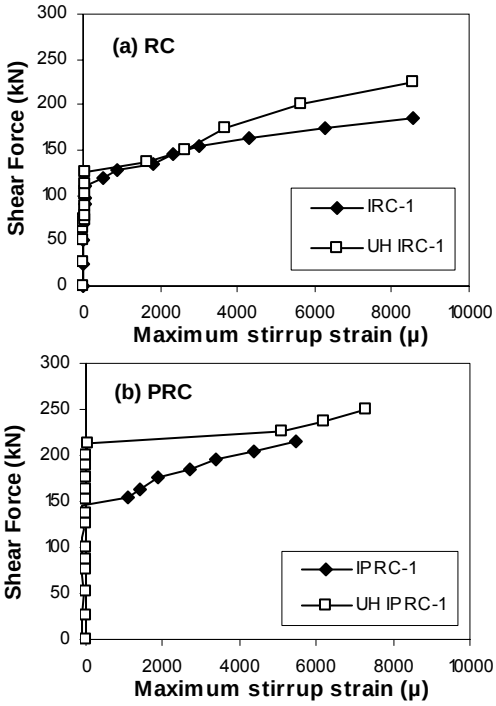

Fig. 6 Load vs. Maximum stirrup strain

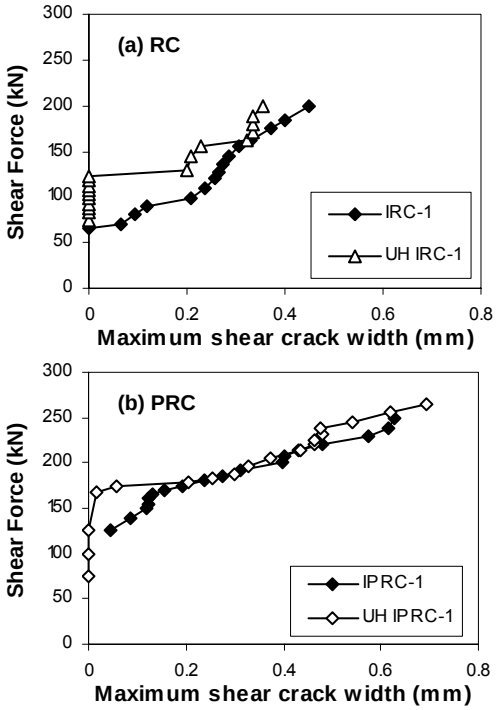

Fig. 7 Load vs. Maximum shear crack width

3.3 Average Distribution of Shear Crack Width in UHSC specimens

Fig. 8 shows the relationship between shear crack width and stirrup strain. Fitting curves obtained from a linear regression analysis represent the relationship between the average values of shear crack width and stirrup strain. For both NSC and UHSC beams, the linear variation between the shear crack width and the stirrup strain determined from the regression analysis shows a reasonable representation of measured data. The average shear crack width variation with increment of stirrup strain is almost same in the both NSC and UHSC of RC specimens while it is smaller in specimen UH IPRC-1. This is due to the fact that provision of prestressing tendon at the mid-depth of section restrained the opening in shear crack width in longitudinal direction. In addition, superior bond characteristics between the UHSC and the steel improve this fact significantly than the NSC specimen. For UHSC specimens, some of cracks may penetrate through aggregates due to strong bond between aggregate and hardened paste, while that of NSC specimen, the cracks always occur in the interface between aggregates and hardened paste. Therefore observed crack plane in NSC specimens was not smooth. The axial compressive force from prestressing (375 kN) in PRC specimens compared to RC specimens caused further reduction in scattering of shear crack width values.

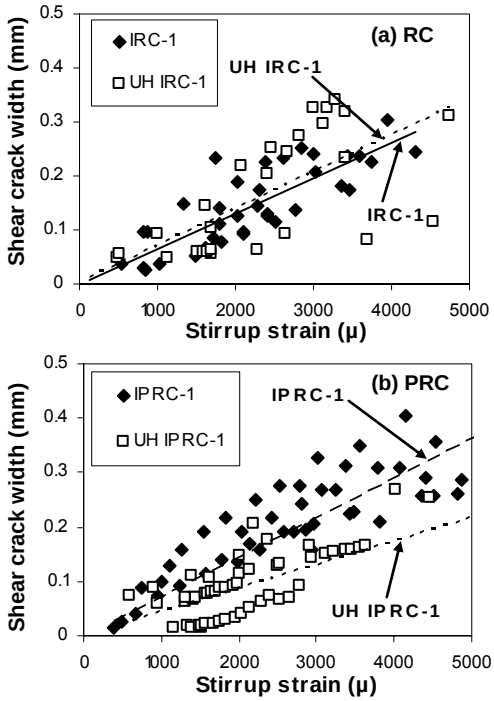

Fig. 8 Average distribution of shear crack width with stirrup strain

3.4 Shear Crack Spacing

Table 5 shows the average shear crack spacing *Smx* and *Smy* (as shown in Fig. 9) for NSC and UHSC specimens. The UH IPRC-1 specimen, which is cast with UHSC, shows comparatively smaller shear crack spacing than the normal strength concrete specimen. This difference is attributed to improvement of bond effect due to high strength concrete with reinforcing steel in UHSC specimen. However, such significant difference could not be seen in normal strength specimen. The smaller shear crack spacing is influenced to smaller crack width in UH IPRC-1 specimen compared to IPRC-1 specimen at the same stirrup strain level (Fig. 8b).

Table 5 Shear crack spacing

Specimen	Horizontal crack spacing, *Smx* (mm)	Vertical crack spacing, *Smy* (mm)
IRC-1	167.00	108.29
UH IRC-1	152.80	79.00
IPRC-1	198.80	203.15
UH IPRC-1	122.80	96.70

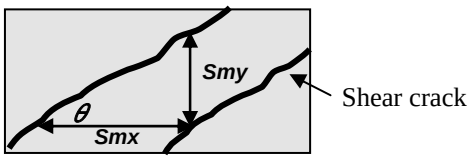

Fig. 9 Interpretation of shear crack spacing

3.5 Distribution of Shear Crack Width

Fig. 10 shows the shear crack width distribution with the increasing load at each stirrup strain gage locations (see Fig. 1 for stirrup strain gage locations). At a single step of load increment, shear crack widths were monitored at the gage locations in the shear span. On the next step, shear crack widths were monitored at the same locations previously measured. It shows that shear crack width data were more scattered in UHSC specimen compared to NSC specimen. Similar scattering of shear crack width data was observed in RC specimens. This is due to the facts that crack localization in UHSC specimen, crack opening inactive due to another crack and properties of aggregates used in the concrete. It has been reported in the literature that the crack plane in high strength concrete is relatively smooth and passes through the aggregate instead of going around the aggregate, as in NSC.

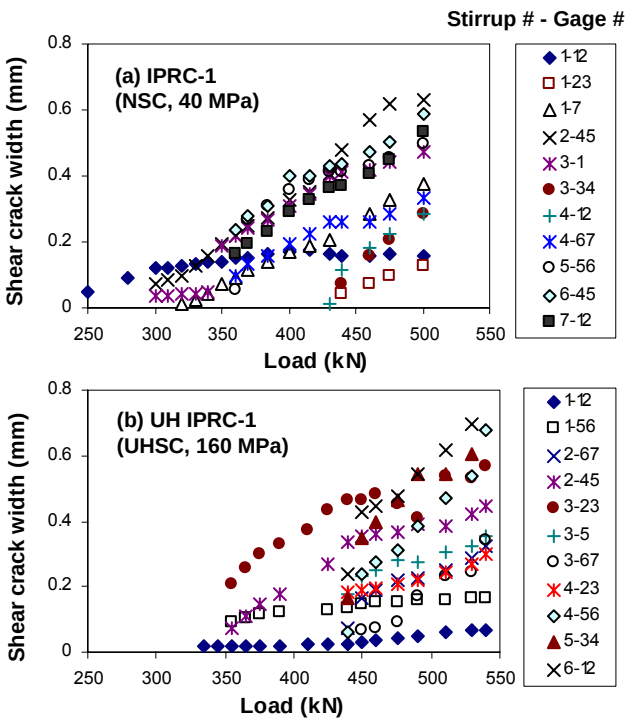

Fig. 10 Distribution of shear crack width

4. NUMERICAL SIMULATION

4.1 Numerical Method

The numerical simulation was carried out using Response-2000 numerical model, which was developed based on the Modified Compression Field Theory (MCFT). Experimental variables and actual compressive strength of concrete of the test specimens were used in the numerical model. The numerical simulation in the model combines a plane section analysis for flexure with the modified compression field theory for shear that accounts for strain compatibility and uses the tensile and compressive stress-strain relationships for diagonally cracked concrete [6]. In this method, the spacing of shear crack was accounted so as to determine shear cracking load and ultimate load. The MCFT that reduces the shear stress was carried for the concrete when large number of shear cracks appeared in the section. The crack spacing is a function of the crack control characteristics of the longitudinal and transverse reinforcement described in the crack spacing model of the numerical program. The sectional analysis was performed at a section located at a distance of 500 mm (approximately at a distance "*d*" and at the section along stirrup location) from the face of the loading point in the shear span. The moment-to-shear force ratio is 0.9 at the selected section. Although the ACI 318-02 code limits the yield stress of shear reinforcement to 400 MPa, the experimentally measured value of yield stress 438 MPa was used in simulation of the model presented here. In addition, constitutional models for concrete and other material were used as described in the numerical program. The material properties of concrete and steel used in the numerical model were based on the experimentally measured values and details provided by manufactures (see Tables 2 and 3).

4.2 Comparison of Load – Mid Span Deflection Relationship

Fig. 11 shows the load mid span deflection relationship for UH IRC-1 and UH IPRC-1 specimens. The prediction of the relationship using numerical program generally showed good agreement with experimental results except at the ultimate failure load in PRC specimen. One of the contributing factors for the lower value predicted by the model at the ultimate load can be the size effect as explained in preceding section. The failure of concrete section occurred due to large local stresses induced at the crack. Further, predicted crack pattern for PRC specimen shows largely distributed crack pattern compared RC specimen. The prediction of flexural cracking load, shear cracking load and load at stirrup yielding agreed well with experimental results. In addition, moment-shear interaction diagram was used to predict the failure mode as discussed in the numerical program [9]. Numerical model well predicted shear failure for all test specimens.

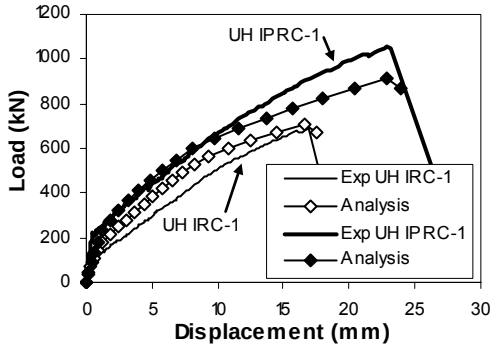

Fig. 11 Load-mid span deflection relationship

4.3 Crack Spacing Model

The shear crack width predicted from this numerical program equals to the product of the average shear crack spacing and principal tensile strain. The crack spacing model based on the CEB-FIP Model code 1978 [6] is:

$$Sm\theta = 2c + 0.1\frac{d_b}{\rho} \qquad (1)$$

where; "c" is the diagonal distance to the nearest reinforcement in the section considered and "d_b" is the diameter of the nearest bar and "ρ" is the percentage of steel. The spacing of the shear cracks depend on the crack control characteristics of both the longitudinal reinforcement and the transverse reinforcement.

4.4 Comparison of Shear Crack Width Values

Fig. 12 compares the relationship between shear force and shear crack width obtained from experimental data and model response predicted from the numerical program Response-2000. The shear crack width values predicted from the numerical program show good correlation with experimental results. In addition numerical program estimated the flexural cracking load, and the shear cracking load very accurately.

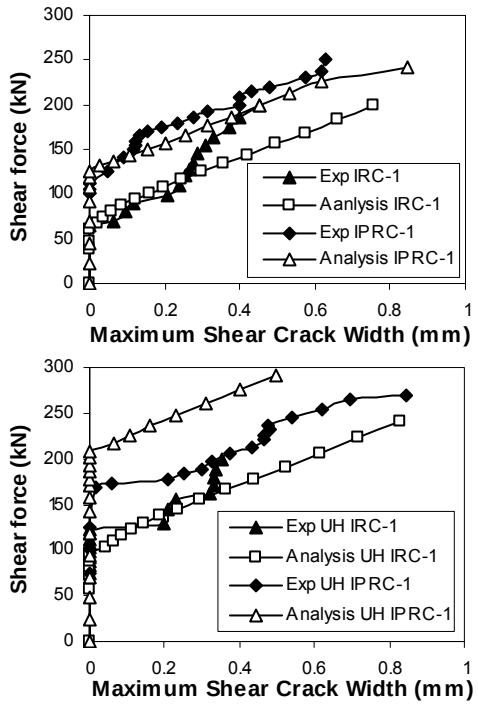

Fig. 12 Comparison of numerical results for maximum shear crack width

5. CONCLUSIONS

The study illustrated an experimental investigation of effect of ultra-high-strength concrete and prestressing force on the shear crack width of I-shaped RC and PRC beams under static loading. In addition, numerical simulation was carried out based on Modified Compression Field Theory (MCFT). The following conclusions are derived from this study:

(1) The ultra-high-strength concrete specimens show larger shear cracking load in RC and PRC specimens compared to normal strength concrete specimens.
(2) After shear cracks appeared, the increment rate in stirrup strain and maximum shear crack width with shear force is similar in both NSC and UHSC specimens.
(3) It was found that the shear crack width variation with stirrup strain in a linear manner in both NSC and HSC specimens. The average shear crack width of UHIPRC-1 is smaller compared to NSC specimen.
(4) The Modified Compression Field Theory based numerical simulation was showed good correlation with experimental results of load deformation response and shear crack width.

REFERENCES

[1] Hussein, N. A., et al., "Effect of Concrete Strength on Long-Term Crack Width of Concrete Members," Proceedings of JCI, Vol. 24, No. 2, July 2002, pp. 1579-1584
[2] Cladera, A., and Mari, A. R., "Experimental Study on High-Strength Concrete Beams Failing in Shear, Engineering Structures," Vol. 28, May 2006, pp. 1825-1834
[3] De Silva, S., et al., "Experimental Study on Shear Cracking Behavior in I-shaped Partially Prestressed Concrete Beams," Proceedings of JCI, Vol. 28, No. 2, July 2006, pp. 817-822
[4] De Silva, S., et al., "Shear Cracking Behavior of High-Strength Prestressed Reinforced Concrete Beams," Proceedings of JCI, Vol. 29, No. 3, July 2007, pp. 679-684
[5] CEB-FIP, "Model Code for Concrete Structures: CEB-FIP International Recommendations," 3rd ed., Paris, 1978, 348 pp.
[6] Bentz, E. C., "Sectional Analysis of Reinforced Concrete Members," PhD dissertation, Dept. Civil Engineering, University of Toronto, Toronto, Canada, 2000